

Harvested area did not increase abruptly – How an inconsistency in satellite-based mapping led to erroneous conclusions

Johannes Breidenbach¹, David Ellison²⁻⁴, Hans Petersson², Kari T. Korhonen⁵, Helena M. Henttonen⁵,
Jörgen Wallerman², Jonas Fridman², Terje Gobakken⁶, Rasmus Astrup¹, Erik Næsset⁶

¹ Department of Forestry and Forest Resources, Norwegian Institute of Bioeconomy Research (NIBIO), Ås, Norway.
Contact: [first_name].[last_name]@nibio.no

² Department of Forest Resource Management, Swedish University of Agricultural Sciences, Umeå, Sweden

³ Land Systems and Sustainable Land Management Unit, Institute of Geography, University of Bern, Bern, Switzerland

⁴ Ellison Consulting, Baar, Switzerland

⁵ Natural Resources Institute Finland (Luke), Helsinki, Finland

⁶ Faculty of Environmental Sciences and Natural Resource Management, Norwegian University of Life Sciences, Ås, Norway

Using satellite-based maps, Ceccherini et al.¹ report abruptly increasing harvested area estimates in several EU26-countries beginning in 2015. They identify Finland and Sweden as countries with the largest harvest increases and the biggest potential effect on the EU's climate policy strategy. Using more than 120,000 field reference observations to analyze the satellite-based map employed by Ceccherini et al.¹ we found that the map's ability to detect harvested areas abruptly increases after 2015. While the abrupt detected increase in harvest is merely an artifact, Ceccherini et al.¹ interpret this difference as an indicator of increasing intensity in forest management and harvesting practice.

Ceccherini et al.¹ use satellite-based Global Forest Change (GFC)² data to estimate the yearly harvest area in each of the EU26-states over the period 2004 to 2018. They report abruptly increasing harvested area estimates in several countries beginning in 2015 and claim this will impede the EU's forest-related climate-change mitigation strategy, triggering additional required efforts in other sectors to reach the EU climate neutrality target by 2050.

We employ more than 120,000 field observations from repeated measurements in 44,000 sample plots from the Finnish and Swedish national forest inventories (NFIs) as reference data in statistically rigorous estimators in order to analyze the accuracy of Ceccherini et al.¹ findings (see Supplement). We find that GFC's ability to detect harvested areas and thinnings* abruptly increases after 2015 (**Figure 1**). When the ability to detect harvest improves, the overall harvested area in GFC will increase, even without a real change in management activity. As a result, more harvested areas and thinnings were detected by GFC after 2015, and this explains why the "harvested area" reported by Ceccherini et al.¹ abruptly increases. In other words, the reported abrupt increase in harvest is to a large degree simply a technical artifact (bias) inherent in the GFC timeseries and not a real-world

*"Thinnings" are forest management activities where typically 20 – 40 % of growing stock is harvested to give more space to the remaining trees to grow before final felling.

37 phenomenon. Their conclusions, however, are the product and direct consequence of an inconsistent
38 time series and are thus both incorrect and misleading.

39 Assuming the average proportion of correctly identified harvested areas before 2015 also applies
40 after 2015, the GFC area after 2015 can be modeled without this increasing sensitivity. This indicates
41 that the GFC recorded increase in “harvested area” of 54% and 36% in Finland and Sweden, reported
42 by Ceccherini et al.,¹ represents an overestimate of 188% and 851% compared to our reference data,
43 respectively (**Figure 2**). Because this modelled area still includes commission error, thinnings and
44 other harvests, additional calculations would be required to provide improved estimates of the
45 actual harvested area change³.

46 In addition to generating harvested area estimates subject to systematic error, Ceccherini et al.¹ do
47 not provide any estimates of uncertainty and further assume all the biomass in their mapped
48 harvested areas was in fact removed. Given that a considerable share of the harvested areas in the
49 period 2016-2018 are thinnings and not final harvests (**Figure 2**), the latter results in even larger
50 errors with respect to C-losses. Ceccherini et al.¹ likewise assume the biomass map they utilize is
51 accurate and without uncertainty, which is unrealistic⁴. We focus on the problems related to the
52 harvested area estimate in Ceccherini et al.¹ as this is the most fundamental issue and is adequate for
53 illustrating the erroneous conclusions drawn by the authors.

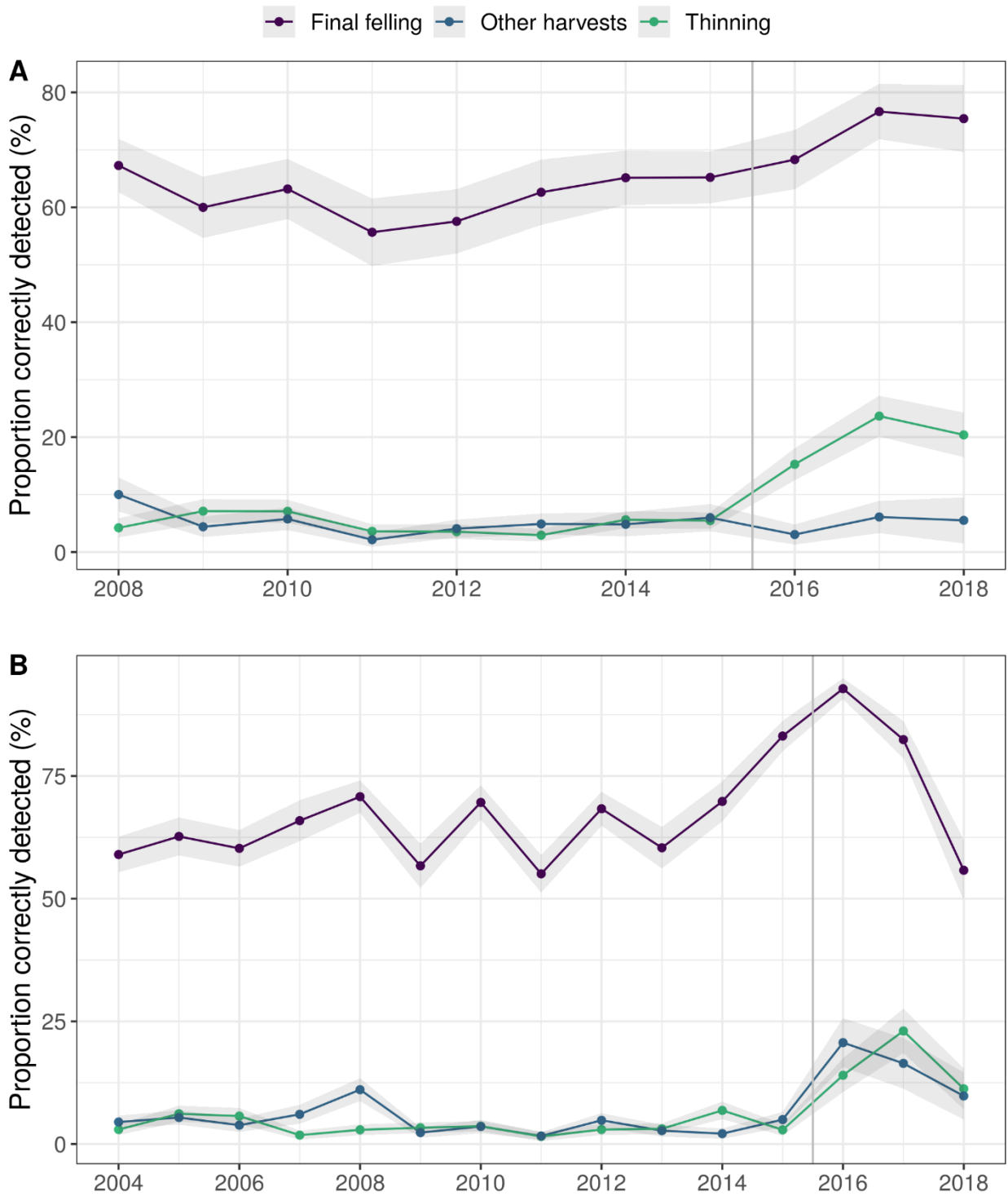
54 Though inconsistencies in GFC’s time series have previously been reported^{3,5}, we acknowledge the
55 strong desire for sound and independently verifiable monitoring strategies driven by their potential
56 for supporting the promotion of forest-related climate benefit⁶⁻⁸. Without this, much hesitation has
57 accompanied interest in mobilizing forest resources behind the climate challenge. Earth observation
58 remote sensing (RS) and related mapping efforts embody the promise of providing very important
59 tools for monitoring land use change, tropical deforestation and forest restoration^{2,9,10}. As such, they
60 likewise hold the promise of supporting efforts to better integrate forest resources into the
61 framework of climate change mitigation strategies.

62 RS products, however, can be used in ways that potentially result in severely biased estimates as we
63 have seen in this study. Because RS data measure reflections of electromagnetic waves (e.g., visual
64 light in the case of optical satellites) rather than the direct object of interest such as forest cover loss
65 and carbon stock, algorithmic models are required for interpreting these reflections. Models,
66 however, are frequently imprecise tools and generally require reference data to correct their data
67 output and thereby provide unbiased estimates^{4,11}. The compilation of RS data results in nice,
68 colorful maps and scientific-looking figures further distract attention. The collection of the required
69 reference data, however, is tedious, expensive and their enormous importance not well
70 understood¹². Combining the GFC map with adequate reference data into reliable estimators can
71 prove very useful for estimating harvested area and related C-stock losses, as illustrated in various
72 studies^{3,5,11,13}.

73 We certainly agree with the authors that one of the more important elements of the Paris
74 Agreement is to; “achieve a balance between anthropogenic emissions by sources and removals by
75 sinks of greenhouse gases in the second half of this century”¹⁴. Based on the data at hand, however,
76 it would be erroneous to lay blame for the failure to achieve these goals at the feet of the forestry
77 sector. We remain hopeful future debate over the role of the European forest sector will remain
78 based on a more scientific foundation.

79

80



81

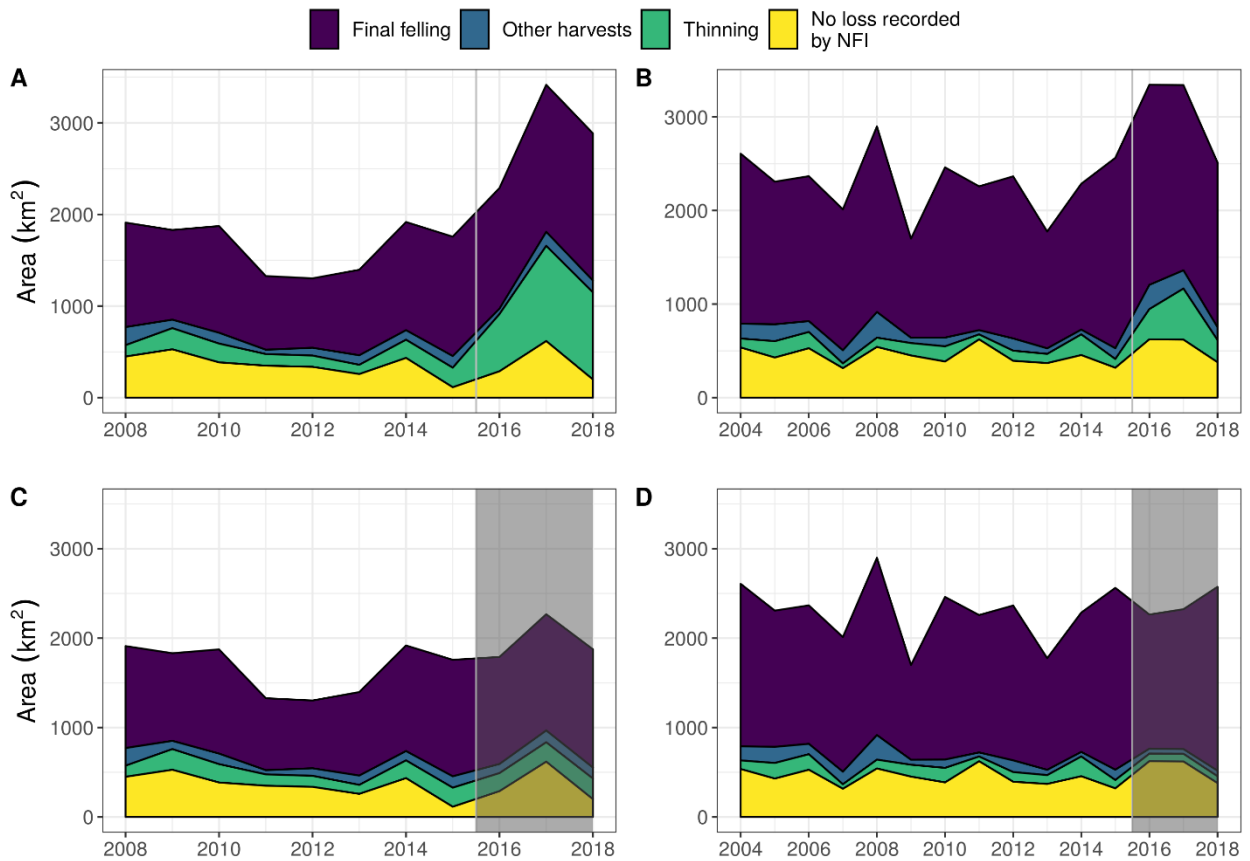
82 **Figure 1: Proportion and 95% confidence interval of correctly detected areas by GFC given change**
 83 **cause as represented by NFI data. A) Finland; B) Sweden.**

84

85

86

87



88

89 **Figure 2: GFC harvested area estimate based on NFI plots with and without correction for an**
 90 **increase in GFC's detection ability after 2015.** The two top figures provide the uncorrected
 91 timeseries of GFC harvested area for A) Finland and B) Sweden along with their field-observed
 92 management outcomes (final fellings, other harvest, thinnings, no management). The area with final
 93 fellings is relatively stable while the area with detected thinnings increases considerably after 2015.
 94 The two bottom figures provide the timeseries of GFC harvested area corrected for GFC's increased
 95 detection ability after 2015 for C) Finland and D) Sweden. For the period 2016-2018, the area is
 96 estimated assuming the correct detection proportion would have stayed the same as before. Based
 97 on these corrected area estimates, there is no abrupt increase in the harvested area after 2015. See
 98 spreadsheet in Supplement for standard errors of estimates.

99

100 [Supplementary material](#)

101

102 [The Finnish NFI](#)

103 The Finnish NFI ¹⁵ is a systematic nation-wide cluster sampling survey composed of permanent and
 104 temporary clusters. In this study, only data from the permanent clusters were used. Since the 10th
 105 NFI (2004-2008), the inventory is continuous with a 5-year cycle such that 20% of the clusters are
 106 measured in each year. Finland is divided into six regions denoted as *strata*, with decreasing sampling
 107 intensity towards the north. In two of these strata, the partly autonomous Åland islands and the low-
 108 productivity, northmost Lapland region, the continuous design is not applied and all plots are
 109 measured in a single field season. Because of this inconsistency compared to the vast majority of the

110 NFI data, these two strata were not included in this analysis. The distance between the permanent
111 clusters ranges from 12 to 20 km.

112 Each permanent cluster consists of 10 – 14 sample plots. Depending on the sampling stratum, a
113 distance of 250 or 300 meters separates adjacent plots. Each sample plot position is recorded with a
114 high-precision Global Navigation Satellite Systems (GNSS) device. Until 2013, the plot design was
115 restricted angle count sampling (ACS) with a basal area factor (BAF) of 2 and maximum radius of
116 12.52 m in southern Finland and a BAF of 1.5 and maximum radius 12.45 m in northern Finland. Since
117 2014, tree-level measurements have been carried out on concentric circular plots with radii of 9.00
118 and 5.56 m for trees with a diameter at breast height (dbh) ≥ 95 mm and ≥ 45 mm, respectively.
119 Trees with a dbh < 45 mm are still sampled using ACS with a BAF of 1.5. As of 2019, the radius of the
120 smaller circle was changed to 4.00 m.

121 A large number of forest stand, site and tree variables are assessed on each plot. The tree level
122 measurements are used to estimate stem volume and biomass. At re-inventory, trees are re-
123 measured and, if logged, harvested trees and time of logging are estimated and recorded. In this
124 study, “logging-type” is defined as; 1) final felling consisting of clear cutting, cutting for natural
125 regeneration and cutting before deforestation, 2) thinning (first thinning and later thinnings), and 3)
126 other harvests (removal of seed trees, salvage cutting tree removal along ditches and other
127 locations). Time of logging is defined by harvest season, not calendar years, and the harvest season
128 starts on the 1st of June.

129 For this study, the last calendar year of a harvest season determined the loss year and forest cover
130 losses have been assessed since 2008 using 33,846 observations from 15,565 permanent sample
131 plots visited from 2009 to 2019. The NFI data used represent a total land area including wetlands of
132 27 Mha.

133

134 The Swedish NFI

135 The Swedish NFI ¹⁶ is a systematic nation-wide cluster sampling survey composed of permanent and
136 temporary clusters. In this study, only data from the permanent clusters were used. The inventory is
137 continuous with a 5-year cycle such that 20% of the clusters are measured in each year. Sweden is
138 divided into five strata, with decreasing sampling intensity towards the north. The distance between
139 clusters ranges from 11 to 26 km.

140 Each permanent cluster consists of 4 – 8 sample plots. Depending on the sampling stratum, a
141 distance of 300 to 1,200 meters separates adjacent plots. Each sample plot position is recorded with
142 a hand-held GNSS device. A consistent plot design has been applied in the time period considered
143 and tree-level measurements are carried out on concentric circular plots with radii of 10.0, 3.5 and
144 1.0 m for measurements of trees with a dbh ≥ 100 mm, ≥ 40 mm and ≥ 0 mm dbh respectively.

145 A large number of forest stand, site and tree variables are assessed on each plot. The tree level
146 measurements are used to estimate stem volume and biomass. At re-inventory, trees are re-
147 measured and, if logged, volume loss, logging type and time of logging are estimated and recorded.
148 In this study, “logging-type” is defined as 1) final felling consisting of clear cutting, cutting for natural
149 regeneration and cutting before deforestation, 2) thinning (first thinning and later thinnings), or 3)
150 other harvests (removal of seed trees, salvage cutting, other tree removal). Time of logging is defined
151 by harvest seasons, not calendar years, where harvest season is defined as the time between the
152 start of the vegetation period (between end of April and end of May, depending on region) in one

153 calendar year to the start of the vegetation period in the next calendar year. The first three harvest
 154 seasons before the measurement of the plot are determined using this method and prior harvests
 155 are grouped into one harvest class.

156 For this study, the first calendar year of a harvest season determines the loss year and forest cover
 157 losses have been assessed since 2004 using 91,304 observations from 28,544 permanent sample
 158 plots visited from 2004 to 2019. The NFI data used represent all of Sweden; a total land area
 159 including wetlands of 45 Mha.

160

161 GFC data and determination of the loss year

162 We intersected the GFC map version 1.6 map used by Ceccherini et al. ¹ with the center coordinates
 163 of the NFI plots. The GFC loss year, if available, was then attributed to the respective NFI period.
 164 Because the NFI-based loss year is estimated, we replaced the NFI loss year by the GFC loss year
 165 where both were observed for individual plots. We use the NFI plots to analyze which changes in the
 166 forest can be detected by GFC. In other words, we use the field observations as ground-truth to
 167 evaluate how well GFC captures harvests over time.

168

169 Estimators

170 The estimators and notation used here closely follow ¹¹ but deviate in important ways when it comes
 171 to the application. The estimators are repeated here for completeness and with minor adjustments
 172 for this context.

173 The estimates utilizing only NFI data are based on the basic expansion (BE) estimator i.e., the sum of
 174 total estimates within each NFI stratum (region)

$$\hat{t}_\tau = \sum_h \hat{t}_h \quad (1)$$

175 where t represents the total of a variable of interest, the “^” identifies this as an estimate of a
 176 population parameter and h indexes the strata. Uncertainty can be estimated by the variance
 177 estimator

$$\hat{V}(\hat{t}_\tau) = \sum_h \hat{V}(\hat{t}_h) \quad (2)$$

178 and the standard error $SE(\cdot) = \sqrt{\hat{V}(\cdot)}$. Estimates in the figures are accompanied by a 95% confidence
 179 interval (CI) calculated as $CI = \hat{t} \pm 2SE(\cdot)$.

180 The total within a stratum is estimated using n_h clusters indexed by i within the sample of clusters s_h
 181 located within the stratum. The design of the NFI clusters is fixed resulting in single-stage cluster
 182 sampling. To simplify the notation and improve readability, we drop the subscript h indexing the
 183 strata using the estimators in this section

184

$$\hat{t}_h = \hat{t} = \lambda \frac{\sum_{i \in s} m_i y_i}{\sum_{i \in s} m_i} \quad (3)$$

185 where λ is the area of the stratum and y_i is the mean over the variable of interest observed on m_i
 186 plots of the i -th NFI cluster. To estimate the population parameter of interest for a certain domain

187 such as the area of final felling in a certain year, a domain indicator variable I_d is used. This domain
 188 indicator is 1 if the plot belongs to the domain of interest and 0 otherwise such that

$$y_i = \frac{\sum_j^{m_i} I_d y_{ij}}{m_i} \quad (4)$$

189 where y_{ij} is the observed value of the variable of interest on the j -th plot of the i -th cluster^{17, p. 65}. In
 190 the case of area estimation, y_{ij} is an n -vector of ones. (In the case where other variables would be of
 191 interest such as carbon stocks, y_{ij} is the observed carbon stock on the plot scaled to per-hectare
 192 values.) The number of plots m_i is typically fixed within a stratum but can vary due to the irregular
 193 shape of the stratum. In other words, m_i is the number of plots on land which usually is constant but
 194 can vary for clusters located close to the coast or along stratum borders.

195 To develop the variance estimator of the total, it is convenient to write the total estimator as

$$\hat{t} = \lambda \hat{Y} = \lambda \frac{\sum_{i \in S} m_i y_i}{\sum_{i \in S} m_i} \quad (5)$$

196 where \hat{Y} is the mean over all plots irrespective of the cluster structure^{17, p. 66}. This is the ratio of two
 197 random variables because m_i is not fixed. Therefore, variance is estimated as

$$\hat{V}(\hat{Y}) = \frac{1}{n(n-1)} \sum_{i \in S} \left(\frac{m_i}{\bar{m}} \right)^2 (y_i - \hat{Y})^2 \quad (6)$$

198 where n is the number of observations (clusters), $\bar{m} = \frac{1}{n} \sum_{i \in S} m_i$ is the average number of plots per
 199 cluster^{17, p. 68}. The variance of the total is then estimated by multiplying the squared area of the
 200 stratum with the variance estimate of the mean

$$\hat{V}(\hat{t}) = \lambda^2 \hat{V}(\hat{Y}). \quad (7)$$

201 We assume simple random sampling and accept that the variance estimates are likely conservative
 202 due to the systematic distribution of the clusters in the NFIs. Other options are possible¹⁸ but will not
 203 generally change our case or conclusions.

204

205 Application of the estimators

206 The loss year determined by GFC if available or otherwise determined by the field crews, was the
 207 primary domain of interest (d). All sample plots that covered a loss year were used for estimating the
 208 variables of interest. For example, for estimates of the domain of interest “final felling area for the
 209 loss year 2018”, all sample plots measured in 2018 and 2019 were used and the indicator variable
 210 was set to 1 for sample plots with loss year 2018 and final felling was recorded based on the
 211 particular logging type. The indicator variable was set to 0 for all other plots. Because GFC
 212 information was not used in this estimate apart from adjustments to the felling year, we refer to this
 213 estimator as \hat{t}_t^{NFI} .

214 Correspondingly, for estimating the area of final felling detected by GFC, the indicator variable was
 215 set to 1 for sample plots with the GFC-based loss year 2018 and final felling recorded as the logging
 216 type. The indicator variable was set to 0 for all other plots. We refer to this estimator as \hat{t}_t^{GFC} .

217 The proportion of correctly detected final fellings (thinnings, or other harvests) by GFC is a ratio of
 218 the two estimates^{17, p. 68}

$$\hat{r}_\tau = \hat{t}_\tau^{GFC} / \hat{t}_\tau^{NFI} \quad (8)$$

219 with variance

$$\hat{V}(\hat{r}_\tau) = \frac{1}{(\hat{t}_\tau^{NFI} / \lambda)^2} \sum_h \hat{V}(\hat{r}_h) (\lambda_h / \lambda)^2 \quad (9)$$

220 where λ_h is the area of the h -th stratum and

$$\hat{V}(\hat{r}_h) = \frac{1}{n_h(n_h - 1)} \sum_{i \in S_h} \left(\frac{m_i}{\bar{m}_h} \right)^2 (y_i^{GFC} - \hat{r}_\tau y_i^{NFI})^2 \quad (10)$$

221

222 where y_i^{GFC} is y_i [eq. (4)] resulting in \hat{t}_τ^{GFC} and y_i^{NFI} is y_i [eq. (4)] resulting in \hat{t}_τ^{NFI} .

223

224 While our approach is suitable for assessing the accuracy of GFC, it is not optimal for estimating
 225 actual harvested area for two reasons. First, the use of the GFC loss year can introduce bias in
 226 estimates if the GFC loss year has a systematic error. Second, official NFI statistics include
 227 measurements from both permanent and temporary sample plots and utilize stand level
 228 observations around the sample plots for area estimation rather than only plot level measurements.
 229 We have employed this approach because plot level measurements conceptually match the pixel-
 230 level GFC data better than stand level observations.

231

232 **Acknowledgements**

233 We thank Dr. Matti Katila (Luke) for extracting the GFC data for the NFI plots of Finland.

234 J.B. was supported by the Norwegian Research Council grant #276398 (INVENT).

235

236 **Author contributions**

237 Conceptualization: D.E., E.N. and J.B.

238 Methodology and Data Analysis: J.B.

239 Data Processing: K.T.K., H.M.H., J.F., J.W., and H.P.

240 Interpretation: All authors.

241 Writing – Original Draft: J.B. and D.E.

242 Writing – Review and Editing: All authors.

243

244 **Competing interests**

245 We declare no competing interests.

246

247 **Data and materials availability**

248 Data and code are available from <https://doi.org/10.5281/zenodo.4625358>.

249

250

251 **References**

- 252 1 Ceccherini, G. *et al.* Abrupt increase in harvested forest area over Europe after 2015. *Nature*
253 **583**, 72-77 (2020).
- 254 2 Hansen, M. C. *et al.* High-resolution global maps of 21st-century forest cover change. *science*
255 **342**, 850-853 (2013).
- 256 3 Rossi, F., Breidenbach, J., Puliti, S., Astrup, R. & Talbot, B. Assessing Harvested Sites in a
257 Forested Boreal Mountain Catchment through Global Forest Watch. *Remote Sensing* **11**, 543
258 (2019).
- 259 4 Næsset, E. *et al.* Use of local and global maps of forest canopy height and aboveground
260 biomass to enhance local estimates of biomass in miombo woodlands in Tanzania.
261 *International Journal of Applied Earth Observation and Geoinformation*, 102138 (2020).
- 262 5 Galiatsatos, N. *et al.* An Assessment of Global Forest Change Datasets for National Forest
263 Monitoring and Reporting. *Remote Sensing* **12**, 1790 (2020).
- 264 6 Bastin, J.-F. *et al.* The global tree restoration potential. *Science* **365**, 76-79 (2019).
- 265 7 Griscom, B. W. *et al.* Natural climate solutions. *Proceedings of the National Academy of*
266 *Sciences* **114**, 11645-11650 (2017).
- 267 8 Brancalion, P. H. *et al.* Global restoration opportunities in tropical rainforest landscapes.
268 *Science advances* **5**, eaav3223 (2019).
- 269 9 Baccini, A. *et al.* Tropical forests are a net carbon source based on aboveground
270 measurements of gain and loss. *Science* **358**, 230-234 (2017).
- 271 10 Harris, N. L. *et al.* Global maps of twenty-first century forest carbon fluxes. *Nature Climate*
272 *Change*, 1-7 (2021).
- 273 11 Breidenbach, J. *et al.* Improving living biomass C-stock loss estimates by combining optical
274 satellite, airborne laser scanning, and NFI data. *Can J For Res*,
275 doi:<https://doi.org/10.1139/cjfr-2020-0518> (2021).
- 276 12 McRoberts, R. E. Satellite image-based maps: Scientific inference or pretty pictures? *Remote*
277 *Sensing of Environment* **115**, 715-724, doi:<https://doi.org/10.1016/j.rse.2010.10.013> (2011).
- 278 13 Turubanova, S., Potapov, P. V., Tyukavina, A. & Hansen, M. C. Ongoing primary forest loss in
279 Brazil, Democratic Republic of the Congo, and Indonesia. *Environmental Research Letters* **13**,
280 074028 (2018).
- 281 14 UN. Paris Agreement. (2015).
- 282 15 Korhonen, K. T. in *National forest inventories - Assessment of Wood Availability and Use*
283 (eds Claude Vidal, Iciar Alberdi, Laura Hernández, & JJ Redmond) Ch. 19, 368-384 (Springer,
284 2016).
- 285 16 Fridman, J. *et al.* Adapting National Forest Inventories to changing requirements – the case of
286 the Swedish National Forest Inventory at the turn of the 20th century. *Silva Fennica* **48**,
287 doi:doi:10.14214/sf.1095 (2014).
- 288 17 Mandallaz, D. *Sampling techniques for forest inventories*. (CRC Press, 2008).
- 289 18 Magnussen, S. *et al.* Comparison of estimators of variance for forest inventories with
290 systematic sampling-results from artificial populations. *Forest Ecosystems* **7**, 1-19 (2020).

291